International Journal of Engineering & Technology, 7 (4) (2018) 4769-4779

International Journal of Engineering & Technology

Website: www.sciencepubco.com/index.php/IJET

Research paper

Hybrid method for brain tumor extraction and MRI scan classification

Moatasem Mohammed Elsayed [1] *, Abeer Twakol Khalil [1], Tamer Omar Mohamed Diab [1], Ashraf Shawky Selim S. Mohra [1]

[1] EE Dept. Benha faculty of engineering Benha , Egypt
**Corresponding author E-mail: moatasem209142@gmail.com*

Abstract

A brain tumor is one of the most devastating diseases. Early detection of brain tumor is a life-saving act. Magnetic Resonance Imaging (MRI) is one of the main techniques to detect brain tumor for diagnosis and treatment. Although there are numerous methods for brain tumor segmentation, automatic and exact segmentation still confronted with some problems and remain one of the most challenging tasks in medical data processing.
This paper presents a machine learning algorithm to classify MRI scans to be normal or abnormal using three techniques of classification which are Support Vector Machine (SVM), Linear Discriminant Analysis (LDA) and Artificial Neural network (ANN) , these techniques of classification are tested on a large database with accuracy of 93.06%, 97.45% and 98.9% respectively, then the detection of the brain tumor region from MRI abnormal scan images is performed using a hybrid method that is based on morphological operations , Filtering and Histogram Processing on images.

Keywords: *Brain Tumor; Histogram Processing; Morphological Operations; MRI Scan Classification; Segmentation.*

1. Introduction

Human body is made up of several types of cells.The Brain is a highly distinctive and sensitive organ of human body. Brain tumor is abnormal growth of cells in the brain [1]. There were an estimated 18.078957 million total cancer cases around the world in 2018, of these 9.456418 million cases were in men and 8.622539 million in women, according to population fact sheet published by international agency for research and cancer [2] , of these total numbers there were 296851 cases for brain and nervous systems cancer with 241037 deaths, that number is even higher for brain metastasis as bladder cancer, breast cancer, kidney cancer, lung cancer, leukemia, lymphoma, and melanoma [3] which presents roughly about 6 million and 32% of the cases , could spread to the brain.
The Magnetic Resonance Imaging (MRI) scan is a powerful scan that produces a detailed image and shows the human internal structure such as organs, bones and other tissues. MRI provides very high resolution images with excellent soft tissue characterization capabilities and gives more sensitive scan image than the Computed Tomography (CT) scan [4].

2. Survey

MRI imaging analysis for brain tumor segmentation is getting attention in recent times due to an increased need for efficient, automatic and exact segmentation. There are large amounts of data. So it is not accepted to analysis it and segment the tumor manually. The work in [5] provided automatic or semi-automatic illustration of the main block diagram used for building up the segmentation method of most algorithms. The presented system structure is the most used structure of brain tumor detection systems and it illustrate how that structure should contain the fundamental four - at least - stages which are first preprocessing stage that might have sub stages like registration , denoising , skull stripping, intensity normalization …etc . Then feature extraction stage which depends on the type of tumor and its grade and those features can either be one single modal based computation (mono-modal) or multi-modal based computation (multi-modal). Highlighting that It is preferred for researchers to combined different features from different modalities due to reach best segmentation results possible. After that segmentation stage which could be region or edge based methods, Classification and clustering took place, then finally Post-processing stage which contained some processes on the resulted image and it also presents Segmentation methods using classification or clustering, grouped by different approaches.
Many Morphological Operations based systems were used for brain tumor extraction, the system in [6] used a method of tumor segmentation from MRI scan images involving gray scale morphological reconstruction , morphological operations and thresholding .With starting by contrast enhancement then cranium removal to avoid the error in segmentation as the intensity of the cranium pixels is comparable to the pixels of the tumor part then the segmentation process is performed, the method in [7] also performed brain tumor extraction using morphological operations into certain steps .The first step was the pre-processing stage and enhancement in which removing noise, removing patient name ,age and other marks in the image took place ,using median filter , Gabor filter ,wiener filter ,Gaussian filter and Sobel filter , Then histogram equalization is used to enhance the quality of the image , The second step was thresholding operation in which a threshold of the image was been calculated using threshold algorithm .The third step was segmentation algorithm in which morphological operations took place such as binary dilation ,binary erosion ,binary

opening and binary closing and then the final step was tumor detection in which the cluster with high intensity pixel was separated, the purposed method in [8] also used thresholding for segmentation and morphological operations as post-processing stage to remove the non-tumor regions detected as false positive by combining erosion and dilation to perform morphological opening , the work in [9] presented techniques and processes used to extract and detect brain tumor from CT and MRI images based on morphological operations ,threshold segmentation and edge detection and it represented also a GUI Matlab based for implementation, Marker controlled watershed segmentation technique is executed in [10] and illustrated that watershed transformation is a powerful and fast technique for both contour detection and region based segmentation. The noise was removed after reading the data using morphological operations such as dilation ,opening, erosion and closing then performing gradient magnitude as a segmentation function, the result was an image and the objects are the foreground and background markers needed to be segmented , then applying watershed transform on gradient magnitude after marking the foreground and calculating the back ground respectively , another algorithm to extract brain tumor area from CT and MRI images illustrated in [11] that used four stages, first image acquisition stage in which preparing and converting the image into gray-scale image then the second stage was for pre-processing with three sub stages applied in which text removal was the first sub stage to remove texts and blurring effect and second sub stage was noise removal using Gaussian filter, average filter and median filter to remove the noise then the last second sub-stage was image sharpening in which Gaussian high pass filter is used and all those sub stages helps detecting edges and improving quality for better results, The third stage was processing stage in which image segmentation take place based on dividing the image into regions only and the fourth and last stage was post processing in which threshold segmentation, watershed transform and morphological operations take place on each region splitted in the previous stage, also an automatic brain extraction methods is illustrated in [12-13] involving region labeling , morphological operations (morphological dilation , morphological erosion) and thresholding for segmentation .

On the other side, Machine learning systems have been developed very fast to solve a lot of problems including in medical data processing field for segmentation and classification, The work presented in [14] first reviewed segmentation and classification techniques for brain tumor from MRI scan images, then proposed a hybrid method - machine learning based - for automatic detection of brain tumor. After illustrating the techniques of segmentation, feature extraction, feature reduction and classification, a Feed-back Pulse Coupled Neural Network technique was chosen for segmentation. The features were extracted using discrete wavelet transform, reduced using Principal Component Analysis. The classification was performed using feed forward back propagation Neural Network. This hybrid method [14] was tested on 101 images consists of 14 normal MRI scan images and 87 abnormal MRI scan images with classification accuracy of 99% , another method to classify a MRI scan images from Harvard Medical School website database [21] is presented in [15] , this method used a wavelet transform for feature extraction , Principal component analysis for feature reduction , and the KSVM to classify the MRI image to be normal or abnormal with four different kernels which are GRB ,LIN ,HPOL and IPOL , also the method in [16] presented an algorithm for brain diagnosis and classification based on higher order statistical texture features and used SVM in classification , the work in [22] was executed involving LDA as a linear classifier , by creating Discriminant analysis model and execute the prediction using posterior probability, prior probability and cost to classify observations by minimizing the expected classification cost , our work of segmentation and classification is performed considering all pervious works.

The organization of the paper is as follows. Section 3 presents the proposed method as it is divided into two flow charts, the first for segmentation and is illustrated from (1 - 4) subsections and the second for classification in the subsection (5). Section 4 presents the result and discussion starting by the segmentation part then the classification part with each followed by the timing for its steps and at the end of the section the timing for all steps from both flow charts. Section 5 presents the conclusion and future work.

3. Proposed method

This paper consists of two main flow charts, the first flow chart in figure 1 is used to detect and extract the brain tumor, the second flow chart in figure 2 is used to classify the image to be either normal or abnormal scan ,each part of this two parts is executed and tested separately , and the segmentation flow chart is then used within the classification flow chart to perform a complete system of classifying the MRI scan and detecting the tumor for abnormal classification class result.

There are two databases that are used to test the segmentation and classification parts, the segmentation flow chart is tested using a collected image scans from [6] [18] which are always abnormal scans to check the accuracy of the segmentation flow chart before using it in the classification flow chart, the classification flow chart is tested using the database [21] which are normal and abnormal scans.

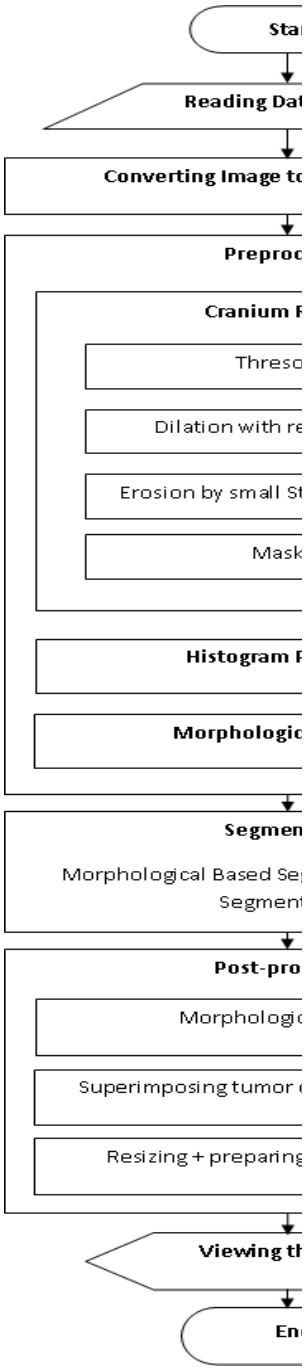

Fig. 1: Segmentation Flow Chart.

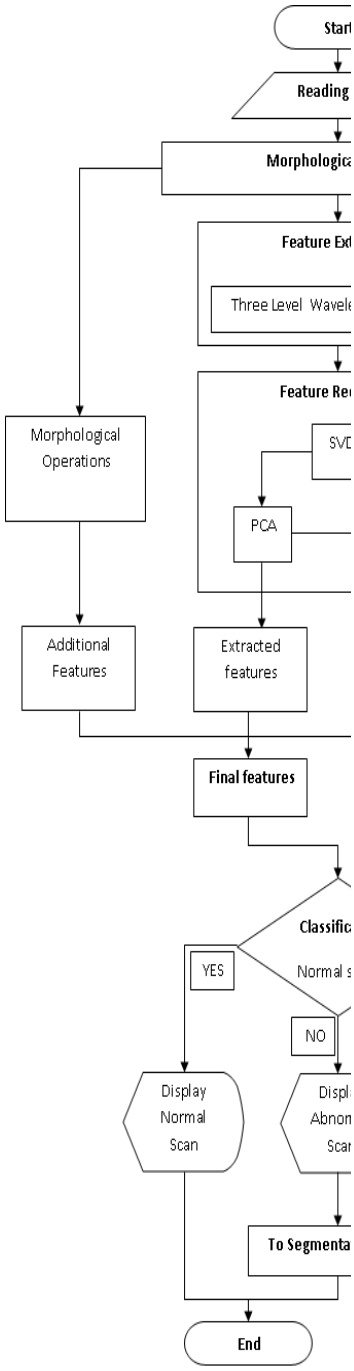

Fig. 2: Classification Flow Chart.

First step is reading the Image as a matrix of size MxN , MRI image is read first as a RGB image , and converted to gray-scale image (each pixel has the intensity between [0-255]) and this step is shown in figure 3.

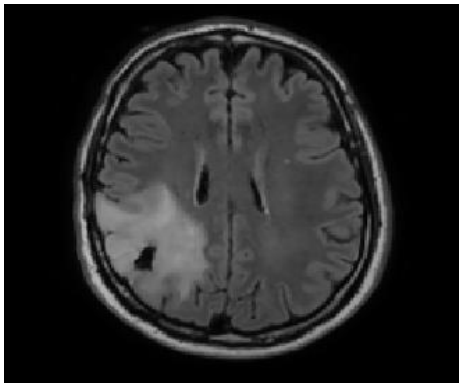

Fig. 3: Viewing the Brain Tumor Image from the Database [6].

3.1. Cranium removal

Staring by the segmentation flow chart, the tumor has higher intensity pixels of the image, but also there are other regions that have comparable intensities to the tumor, those regions are the Skull pixels, so the next step is to remove the skull part to avoid error in segmentation. This process is executed by cropping the undesired regions in the image which involves thresholding technique as a primary step to result a binary image that has the shape of the skull by assigning the threshold with the value of skull pixels; this threshold process is given by:

$$g(x,y) = \begin{matrix} a \text{ if } f(x,y) > T \\ b \text{ if } f(x,y) \leq T \end{matrix} \quad (1)$$

Where object or foreground pixels are labeled as (a), and background pixels are labeled as (b), for binary image [a=1 (white), b=0 (black)], $f(x,y)$ is the input image and $g(x,y)$ is the output image.
Morphological operation for region filling (repeated dilation with reconstruction) is given by:

$$X_K = \left((X_{K\_1}) \oplus B\right) \cap A^C \quad (2)$$

Where X_K is assigned first as a marker image and then assigned to the output of each repeated process, B is the structure element and A^C is the complement of the original iamge.
An erosion process is used to result an image suitable for the masking process. The dilation and erosion processes on that resulted binary image is given by:

$$A \oplus B = \{z|(\dot{B})z \cap A \neq \emptyset\} \quad (3)$$

$$A \ominus B = \{Z|(B)z \cap A^C = \emptyset\} \quad (4)$$

Where A is original image set, B is the structure element, $\emptyset$ is the empty set and the process over all points z.
By that the skull is removed from the original image and the result will be the inside of the skull as shown in figure 4.

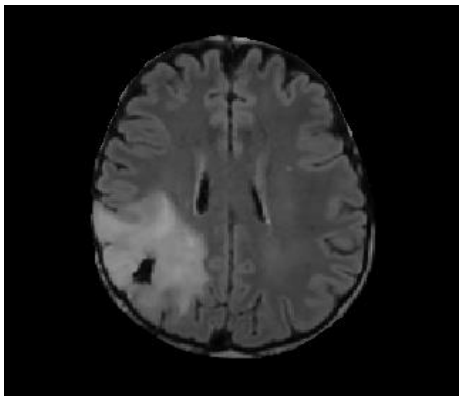

Fig. 4: Viewing A Skull Removed Brain Tumor Image.

3.2. Preprocessing step

After the skull is removed , a preprocessing stage is taking place ,in which histogram specification of the best result image is applied on the image as an automatic enhancement process , which is the process of histogram equalization but to a specific extend that is the processed output image needed to be approximately similar to it, This specific extend is assigned from trying the best image result in

any database and used as reference ,by that the manual adaptively is not used , this process is given from the equations:

$$S = T(r) = (L-1)\int_0^r Pr(w)\,dw \quad (5)$$

$$G(z) = (L-1)\int_0^z Pz(t)dt = s \quad (6)$$

$$z = G^{-1}(s) \quad (7)$$

Where r & z are two continuous intensities , t & w are the dummy variables of integration, P is the histogram distribution probability and (L-1) is used to convert from probability value (which in between 0 - 1) to gray scale value again(L=256).
Which means that z is obtained from s (mapping from s to z) by equalizing the input image (mapping from r to s) then performing the inverse mapping (from s to z), which gives the most close output possible to the desired histogram. Then Gray scales morphological operations with reconstruction are performed on the image (Morphological Filtering) to uniform the background, removing false positives and false negatives, filling the holes and removing the undesired group of pixels, the gray scale dilation, erosion, opening and closing is given by the following equations:

$$(f \oplus b) = Max\{f(x-\dot{x}, y-\dot{y}) + b(\dot{x},\dot{y}) | (\dot{x},\dot{y}) \in D_{\dot{b}}\} \quad (8)$$

$$(f \ominus b) = Min\{f(x+\dot{x}, y+\dot{y}) - b(\dot{x},\dot{y}) | (\dot{x},\dot{y}) \in D_{\dot{b}}\} \quad (9)$$

$$f \circ b = (f \ominus b) \oplus b \quad (10)$$

$$f \cdot b = (f \oplus b) \ominus b \quad (11)$$

Where f is the Gray Scale image, b is the structure element and where D_b is the domain of b, and f(x, y) is assumed to equal $-\infty$ outside the domain of f.
The result image from these processes is shown in figure 5.

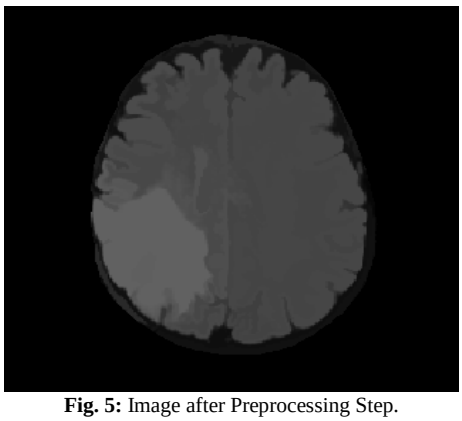

Fig. 5: Image after Preprocessing Step.

3.3. Segmentation process

As now the cranium is removed, segmentation process that morphologically based can now take place, the maxima intensity values are the tumor part with some regions in addition that could be caused from noise or something else, so, using the value of the tumor pixels as a threshold to convert the image to binary image as (1) is assigned to the tumor pixels and (0) is assigned to every other pixel. The result image now has the tumor part extracted and some non-tumor pixels or regions (group of pixels), smoothing morphological filtering (Open close filtering – Close Open filtering – Open Close filtering with increasing structure element), region filling by a suitable structure element, and morphological operations are used to eliminate all the other undesired pixels or regions, this step is shown in figure 6.

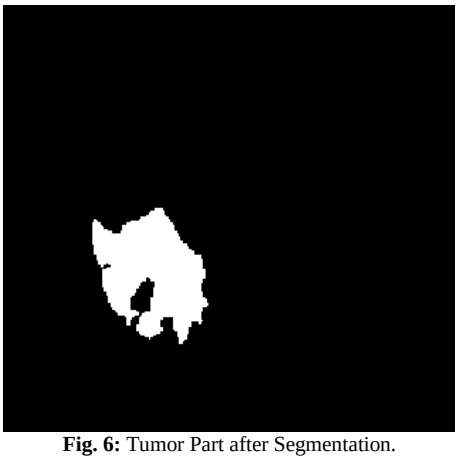

Fig. 6: Tumor Part after Segmentation.

3.4. Post processing step

Now the tumor part is only detected, but the original image has many changes, the next step is to superimpose the detected tumor part on the original image, and this step will result the original gray-scale image with a white tumor part superimposed on it, which is the detected tumor part, this step is shown in figure 7.

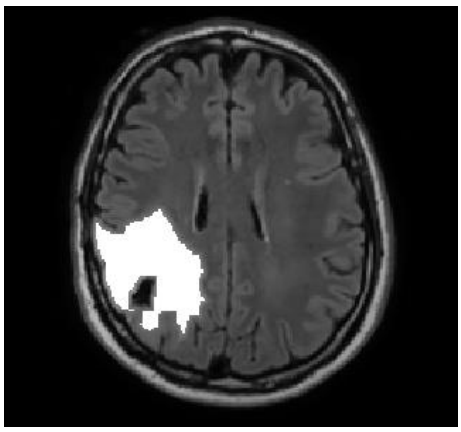

Fig. 7: Superimposing the Tumor on the Original Image.

3.5. Tumor classification

The classification flow chart is applied on the images from the database [21]. The First step is to read the image ,then extracting the features of this image using three level wavelet decomposition technique to perform Dyadic portioning , and using the approximation image at level three as an input to data analysis step next .
Scaling filter image is given by:

$$W_\phi(j_0,k_1,k_2) = \frac{1}{\sqrt{N_1N_2}} \sum_{n_1=0}^{N_1-1}\sum_{n_2=0}^{N_2-1} S(n_1,n_2)\phi_{(j_0,k_1,k_2)}(n_1,n_2) \quad (12)$$

Where n_1, n_2 are for image domain indexes, k_1, k_2 are wavelet filter domain indexes, $S(n_1,n_2)$ is the image signal, j_0 is the scale, $\phi_{(j_0,k_1,k_2)}(n_1,n_2)$ is the filter applied on the n_1, n_2 position of the image. Meaning at every point of the image $S(n_1,n_2)$,applying the corresponding filter and the product of $S(n_1,n_2)\phi_{(j_0,k_1,k_2)}(n_1,n_2)$ is added up to give $W_\phi(j_0,k_1,k_2)$.
Similarly, wavelet filter images are given from:

$$W_\psi^i(j_0,k_1,k_2) = \frac{1}{\sqrt{N_1N_2}} \sum_{n_1=0}^{N_1-1}\sum_{n_2=0}^{N_2-1} S(n_1,n_2)\psi^i_{(j_0,k_1,k_2)}(n_1,n_2) \quad (13)$$

$i = \{H, V, D\}$

Where (H) is the LPF on the columns and HPF on the rows, (V) is the HPF on the columns and LPF on the rows, (D) is the HPF on the columns and HPF on the rows.
The following figure shows the three level wavelet decomposition processes.

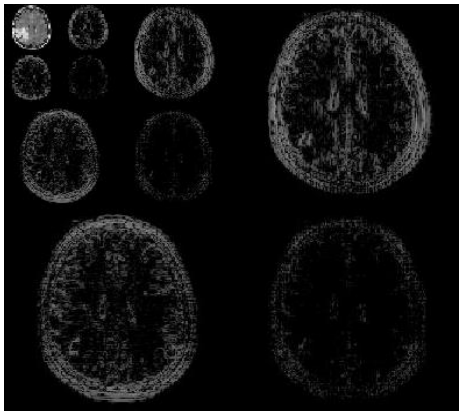

Fig. 8: Three Level Wavelet Decomposition Images.

The next step is feature reduction by applying the (PCA) principal component analysis on the approximation image involving (SVD) singular value decomposition [20].
Which gives:

$$A = \hat{U} \hat{\sum} V^* \quad (14)$$

Where:
U is a m × m unitary matrix over K (if K = R, unitary matrices are orthogonal matrices), Σ is a diagonal m × n matrix with non-negative real numbers on the diagonal, V is a n × n unitary matrix over K, and V* is the conjugate transpose of V. Assuming a data matrix X using SVD as it decomposes any matrix to three main parts as shown previously from equation (14) and after calculating U and introducing a new set Y to be:

$$Y = U^* X \quad (15)$$

$$C_Y = \frac{1}{n-1} Y Y^{-1} = \frac{1}{n-1} \sum^2 \quad (16)$$

And the covariance matrix for the new frame of reference (as it is the rotation of X) is given by:
By taking a data matrix and decompose it using SVD and using the U to transform X to a frame of reference Y where the covariance matrix C_Y is diagonal which leads to redundant free data. After applying PCA on the wavelet decomposition output , the result is used to extract some feature , and then generating Gray Level Co-occurrence Matrix (GLCM) that is used to extract more features, and the result number of features after these processes is much less than the one resulted from wavelet directly and redundant free . The next step is to use those features to train the classifiers, and for best results first the slice image classification is used then the classifications is applied on the scan type, and train each classifier at each level. Additional features are applied to improve the performance. These features are extracted from the binary image resulted from segmentation and it is morphologically based to help improve classification results.

3.6. Techniques used for classification

The Experiment of tumor classification is carried out using three techniques which are Support Vector Machine (SVM), Linear Discriminant Analysis (LDA) and Artificial Neural Network (ANN).

3.6.1. Support vector machine (SVM)

The decision rule of the SVM, assuming that there are two classes, A and B, class A contains the positive samples and class B contains the negative samples, is given by:

$$\sum_i \alpha_i y_i \bar{X}_\iota \cdot \bar{u} + b \geq 0 \; For\ positive\ samples \quad (17)$$

Where the decision rule is dependent – and only dependent –on the dot product of the sample vectors $\bar{X}_\iota$ and the unknown vector $\bar{u}$, Figure 9 Shows how the distance between margins is calculated which is involved in the determination of the decision rule.

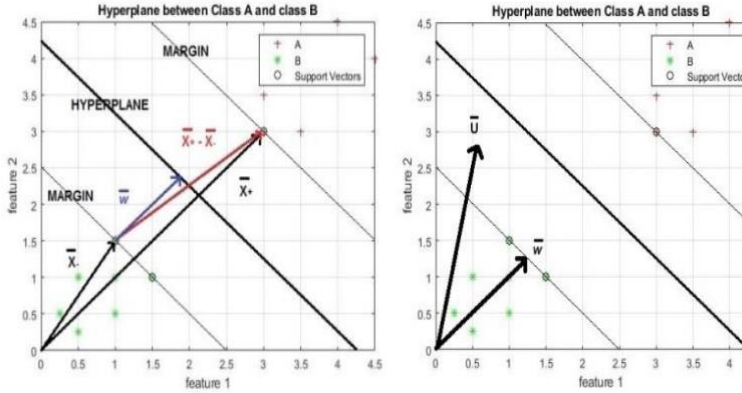

Fig. 9: On the Left (Shows How the Width between Margins Is Calculated) on the Right (Shows How the Unknown Vector U Is Classified Depending on the Projection on the Normal Vector W).

For nonlinearly separable problems, a transformation is required to transfer the samples into new space in which the data set is separable, this transformation $\emptyset(X_i)$ is performed by the transformation of one vector dot product with the transformation of another vector as:

$$\emptyset(\bar{x}) \cdot \emptyset(\bar{y}) \quad (18)$$

$$\emptyset(\bar{x}_i) \cdot \emptyset(\bar{x}_j) \quad (19)$$

$$K(x_i, x_j) = \emptyset(\bar{x}_i) \cdot \emptyset(\bar{x}_j) \quad (20)$$

The function K is the kernel function, which provides the dot product of those two vectors $\bar{x}_i$, $\bar{x}_j$ in another space where the samples are linearly separable, figure (10) shows a simple example of nonlinearly separable samples of two features and figure 11 shows how those samples are separable after applying the kernel function then using SVM to separate these samples.

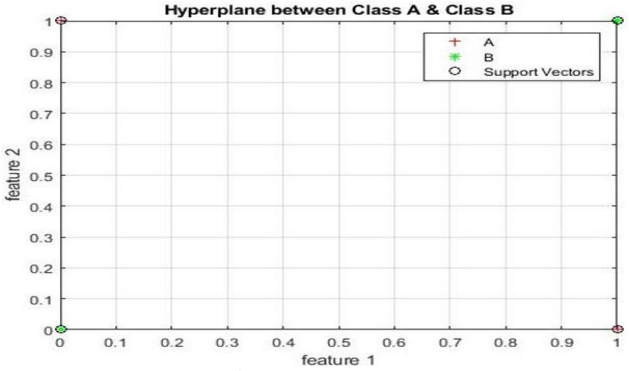

Fig. 10: An Example of Samples That Is Not Linearly Separable.

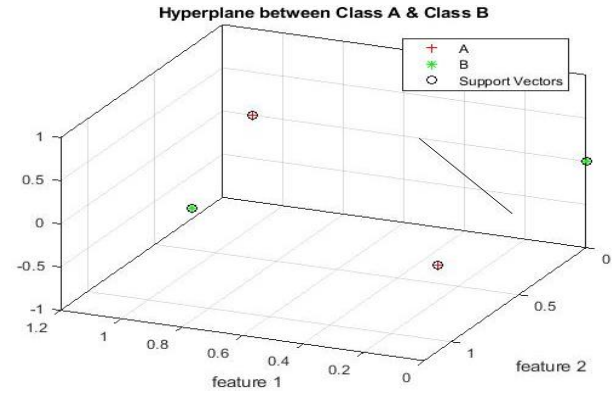

Fig. 11: Samples are Linearly Separable after Applying Kernel Function (KSVM).

SVM used in this paper with a linear kernel, then it is repeated using Gaussian Radial Basis Function kernel which is given by:

$$K(x, \acute{x}) = exp(-\frac{\|x-\acute{x}\|^2}{2\sigma^2}) \quad (21)$$

Where $\|x - \acute{x}\|^2$ is the squared Euclidean distance and σ is a free parameter.

3.6.2. Linear discriminant analysis (LDA)

LDA is used as an LDA classifier, by creating Discriminant analysis model and execute the prediction using posterior probability, prior probability and cost to classify observations by minimizing the expected classification cost [22], with the classes assumed to have the same co-variance matrix to perform a linear classifier, but the co-variance matrix is inversed using the Pseudo inverse in the decision rule determination. The LDA classifier minimizes the expected classification cost as:

$$\hat{y} = arg\, min_{y=1,\ldots,K} \sum_{k=1}^{K} \hat{P}(k|x) C(y|k) \quad (22)$$

Where $\hat{y}$ is the predicted classification, K is the number of classes, $\hat{P}(k|x)$ is the posterior probability of class k for observation x, $C(y|k)$ is the cost of classifying an observation as y when its true class is k.

3.6.3. Neural network

The Neural Network used is Pattern Recognition Feed-forward Multilayer Perceptron Network; the network structure is shown in figure 11.

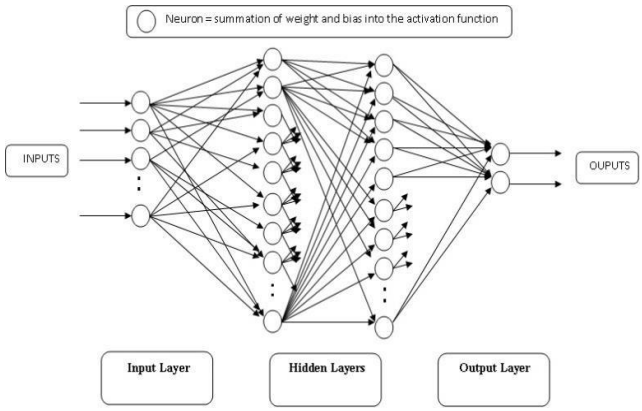

Fig. 12: Shows the Structure of the Neural Network.

The output of the k+1 layer of the j^{th} neuron is given by:

$$x_j^{(k+1)} = R\left(\sum_{i=0}^{Mk} W_{ij}^{(k+1)} x_i^k\right) \quad (23)$$

Where x_i^k is the output of the i^{th} neuron in the K^{th} layer, R is the activation function, W is the weight connections between neurons, Mk is the number of nodes in the K^{th} layer, meaning that the output of the j^{th}neuron in the (k+1) layer is the nonlinear function of the weighted sum of the output of all the neurons in the K^{th} layer, and the error function that is minimized during training is given by:

$$E = \frac{1}{2}\sum_{j=0}^{Mk}(x_j^k - d_j^k)^2 \quad (24)$$

Where x_j^k is the output of the j^{th}neuron in the k^{th}layer, and d_j^k is the target output of the j^{th}neuron in the k^{th}layer.

The Neural Network used for MRI scan image classification is a Pattern Recognition Feed-forward Multilayer Perceptron Network that consists of two hidden layers of 16 neurons in the first hidden layer and 8 neurons in the second hidden layer using two types of activation function (tan-sigmoid and ReLU) in both hidden layers providing the nonlinearity , an output layer with Softmax classification function with two neurons presenting the two classes which performs Multinomial Logistic Classification ,then this network is trained , tested and validated using the 274 slice images [21] as 70% training 15% validation and 15% testing , figure 13 shows the diagram of the network . The number of hidden layers and the activation function are selected based on the result shown in the result section.

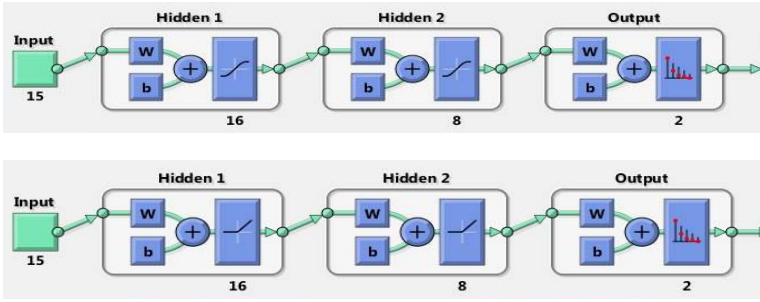

Fig. 13: Neural Network Diagram (In the Top: NN with Tan-Sgmiod Activation Function for the Hidden Layers - the Second Diagram Shows NN with Relu Activation Function for the Hidden Layers)

The training is performed using various techniques ,these techniques are (Gradient Descent Algorithms - Conjugate Gradient algorithms - Quasi-Newton Algorithm - and Bayesian Regularization Back-Propagation Algorithm), in section IV , table 3 shows the result of using these techniques to train the network .

4. Results and discussion

Binary classification is used to evaluate this algorithm of segmentation [17], and this could be done depending on the following table:

Table 1: Binary Classification

	Tumor Positive	Tumor Negative
Segmented positive	A (True positive)	B (False positive)
Segmented negative	C (False negative)	D (True negative)

A, B, C and D are used to calculate segmentation characteristics which are (Sensitivity - Specificity - Precision or positive predictive value - Negative predictive value - Accuracy) and are given by:

$$Sensitivity = \frac{A}{A+C} \quad (25)$$

$$Specificity = \frac{D}{D+B} \quad (26)$$

$$\text{Positive predictive value} = \frac{A}{A+B} \quad (27)$$

$$\text{Negative predictive value} = \frac{D}{D+C} \quad (28)$$

$$\text{Accuracy} = \frac{A+D}{A+B+C+D} \quad (29)$$

4.1. Viewing the results on GUIs

The first GUI shown in figure 14 is for applying the segmentation flow chart on a selected image from the database [6] using Matlab.

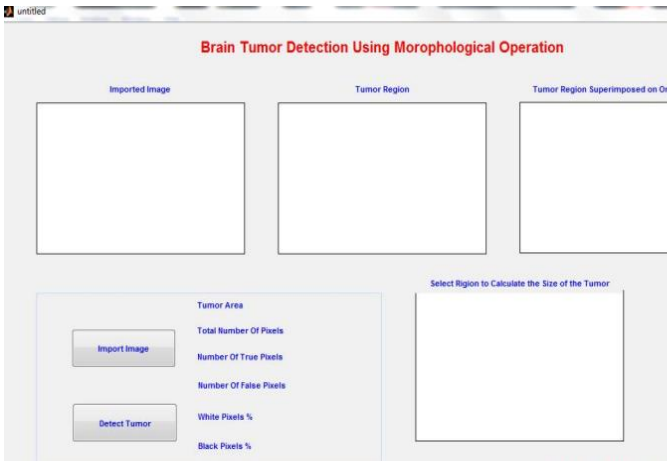

Fig. 14: GUI for Brain Tumor Detection.

First selecting the image from the database as shown in figure 15.

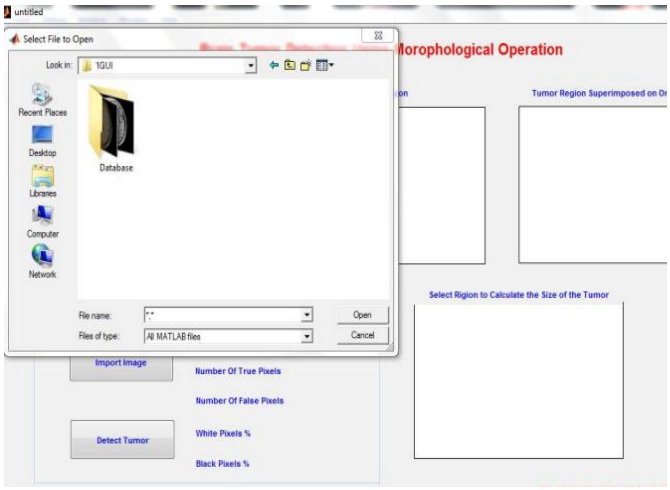

Fig. 15: Selecting Image from the Database.

For more than one tumor part , a dialog box appears asking for the tumor part to calculate its size , as the method of segmentation detects all tumor parts and if there are more than one part (i.e. separated two parts) a labeling method is used to number any part to be detected as a tumor and ask for the number of the object then the size of the tumor is calculated ,this step shown in figure 16.

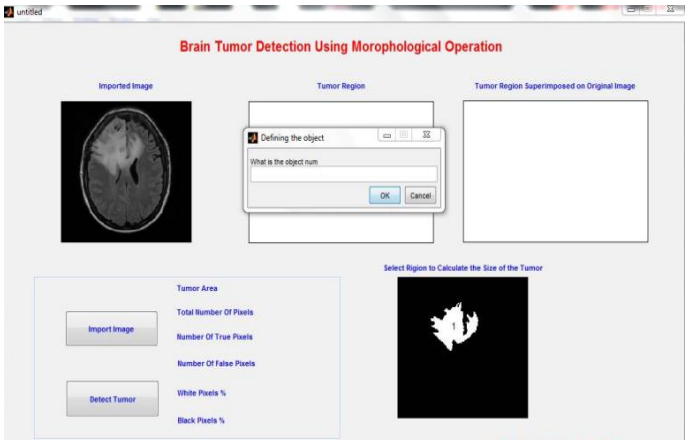

Fig. 16: Reading the Selected Image.

The result images appear as "Tumor region" and "Tumor region superimposed on the original image", this is shown in figure 17.

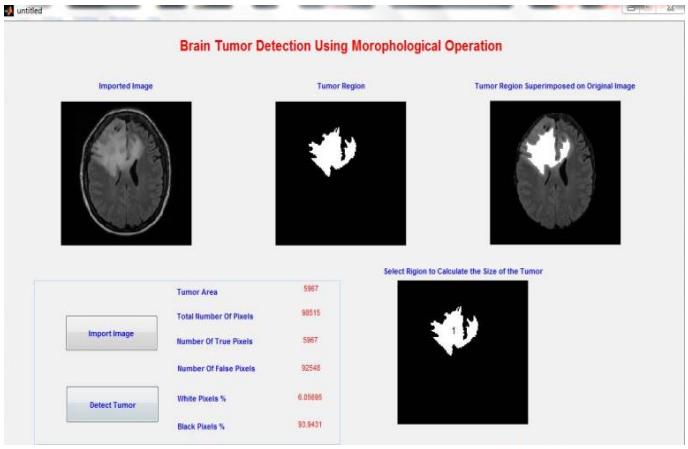

Fig. 17: Segmentation Results.

The Next GUI shown in figure 18, 19 is used for reading 6 images in one step from the segmentation database [6] [18] and applying the binary classification on them, then it provides (TPR (true positive ratio) - TNR (true negative ratio) - PVP (predictive value positive) - A (accuracy)).

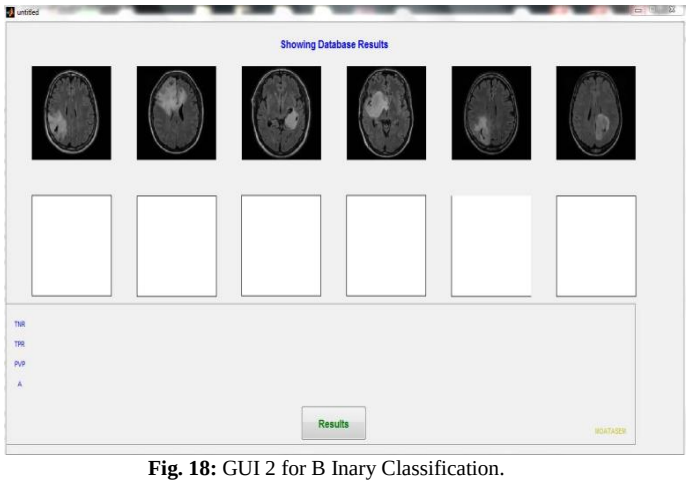

Fig. 18: GUI 2 for B Inary Classification.

Fig. 19: Viewing the Results.

The following diagram in figure 20 shows the binary classification for 10 images from the segmentation database [6] [16] that are used to test the segmentation method as a primary test using (TPR (true positive ratio) - TNR (true negative ratio) - PVP (predictive value positive) - A (accuracy)).

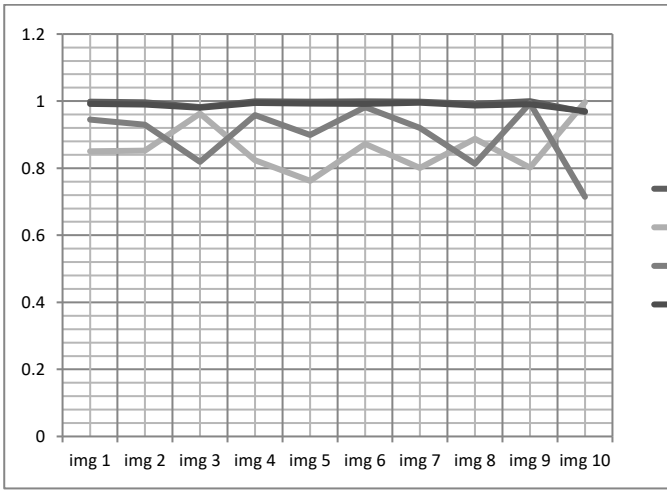

Fig. 20: The Binary Classification (TPR-TNR-PVP-A).

Also the following diagram in figure 21 shows the difference between applying the segmentation directly on the image without all preprocessing stages which result failure in some images and applying all the methods on the images by measuring (TPR (true positive ratio) - TNR (true negative ratio) - PVP (predictive value positive) - A (accuracy) for both cases.

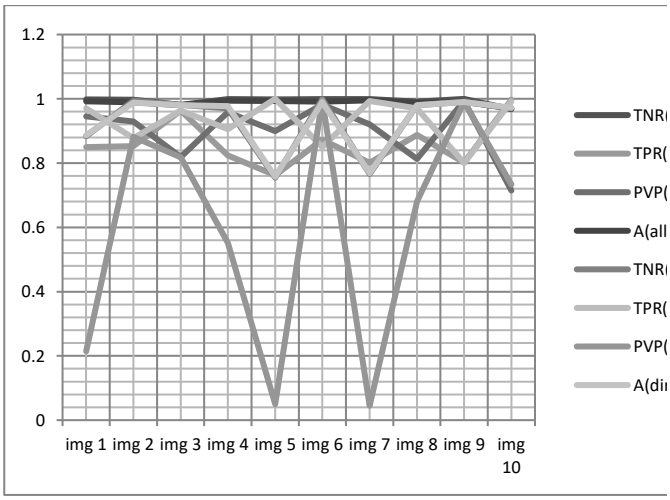

Fig. 21: Difference between Direct Segmentation and the Provided Method.

Measuring (TPR (true positive ratio) - TNR (true negative ratio) - PVP (predictive value positive) - A (accuracy) for both cases with average accuracy for the proposed method of 98.84% than 92.9% for direct segmentation of collected images from databases [6] [18] for testing the segmentation only.

The following diagram in figure 22 shows how much time each step in the segmentation flow chart take to be executed (Using a laptop with processor Intel(R) Core(TM) i3-6006U @2.00GHz 4GB RAM).

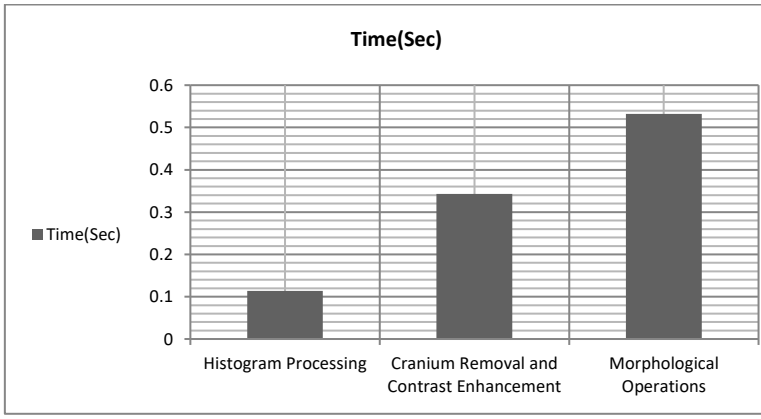

Fig. 22: Shows the Time Duration Spend by Each Step (Brain Tumor Extraction Part).

4.2. Results from brain tumor segmentaion and classification parts (all method)

The result presented in [14] is 101 images used to classify the MRI scan images to be either normal or abnormal scan with 99% accuracy , In this paper 274 slice image [21] is used to train and test the classifiers and the results is shown in table 2.

Table 2: Setting of Training and Test Images

Total Number of Images	Classification Technique			
	SVM		LDA	Neural Network
274 Images (13 Normal - 261 Abnormal)	Linear Kernel 70.40%(199 of 274 Images)	RBF Kernel 93.06% (255 of 274 Images)	97.45%(267 of 274 Images)	98.9% Average Total Confusion Matrix(271 of 274 Images)

The implementation of SVM and LDA classification techniques is shown in figure 23.

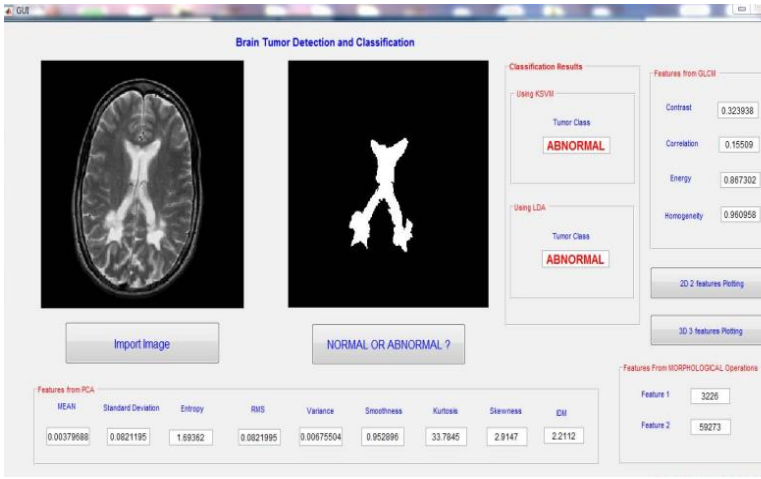

Fig. 23: Shows A GUI of Implementing SVM and LDA Techniques.

Which shows the features extracted from the MRI scan image and the classification result for both SVM and LDA, the GUI also has "2D 2 feature plotting" for plotting each two features of the training features against each other in a 2D diagram, and a "3D 3 feature plotting" for plotting each three features of the training features against each other in a 3D diagram , with both cases showing the hyper-plan (a line in the 2D plotting diagram and a plane in the 3D plotting diagram) as shown in the following figure.

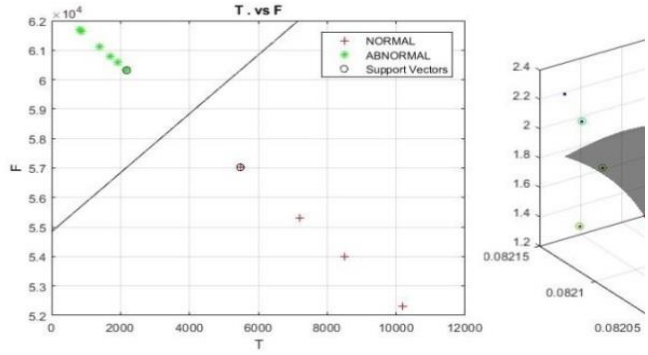

Fig. 24: 2D 2 Feature Plotting & 3D 3 Feature Plotting (Using Matlab).

A sample of MRI brain scan images from the database [21] before and after the segmentation process is shown in figure 25, this segmentation process is executed after the classification process first executed and indicated that these scans are abnormal scans.

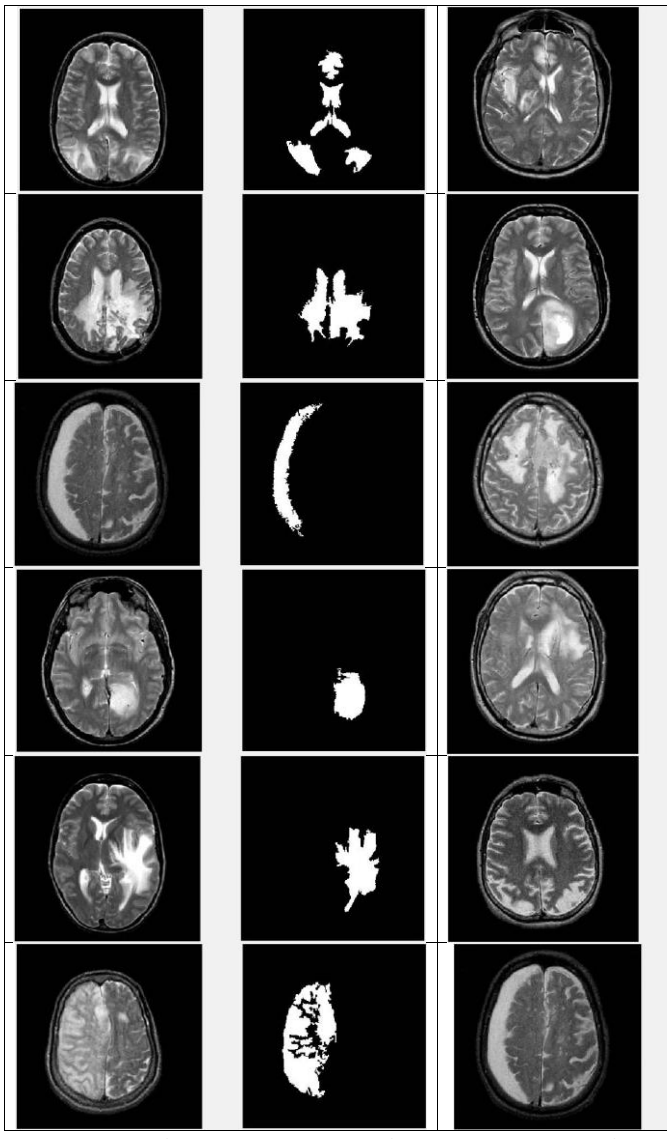

Fig. 25: Sample of MRI Brain Scan Images from the Database [21] before and after the Segmentation.

The result confusion matrices that determined from using the neural network is shown in figure 26, also ROC diagram is shown in figure 27.

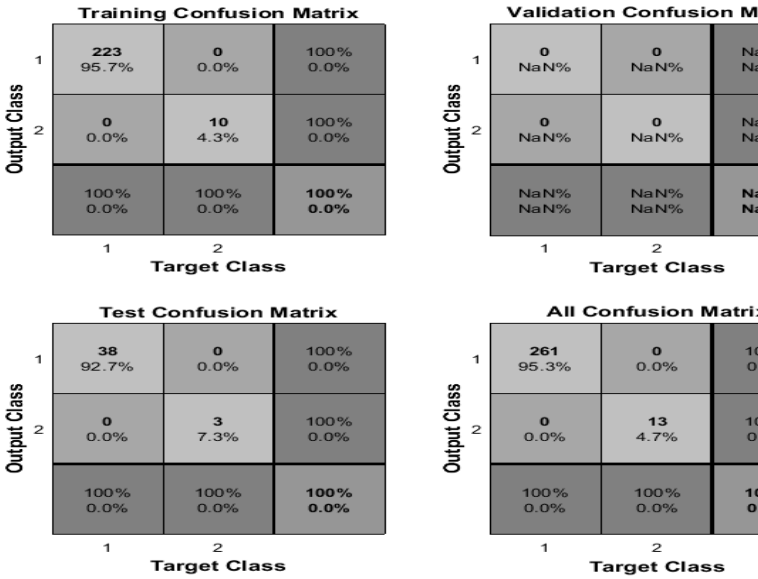

Fig. 26: Shows the Confusion Matrices (Best Result).

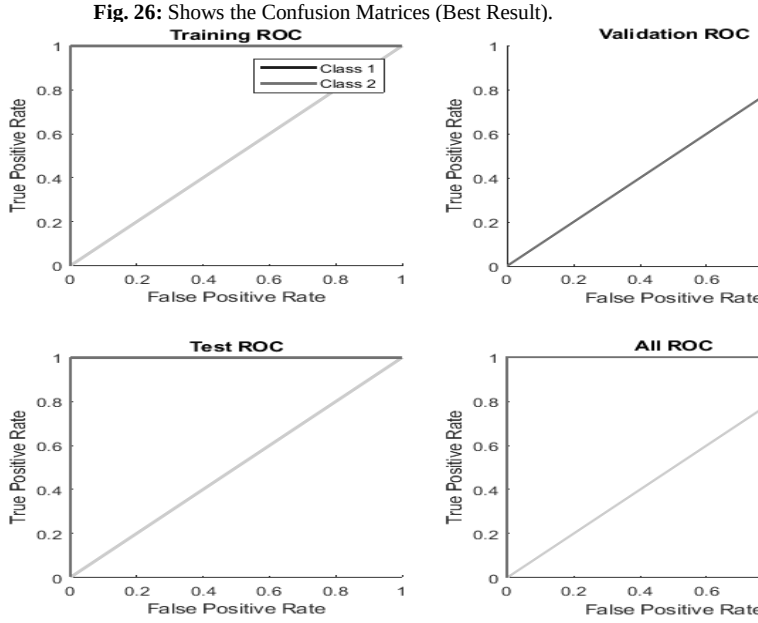

Fig. 27: ROC Graphs (Best Result).

The training techniques that are used for the network are as follows:

Gradient Descent Algorithms
1) Gradient Descent back-propagation.
2) Gradient Descent with Momentum.
3) Resilence back-propagation.

Conjugate Gradient Algorithms
1) Scaled Conjugate Gradient.
2) Conjugate Gradient back-propagation With Fletcher-Reeves Updates.
3) Conjugate Gradient back-propagation With Polak-Riebre Updates.

Quasi Newton
1) BFGS Broyden Fletcher Goldfarb Shanno algorithm.
2) Levenberg-Marquardt back-propagation.

Bayesian Regularization
1) Bayesian Regularization Back-propagation

The average results of using these techniques are shown in table 3.

Table 3: Training Algorithms with Results

Algorithm	Type	Activation	Epoch	Classific-

		Function		ation %
Gradient Descent	Gradient Descent back-propagation	Tan-sigmoid	1000	95.3%
		ReLU	207	95.3%
	Gradient Descent with Momentum	Tan-sigmoid	1000	95.3%
		ReLU	1000	94.9%
Conjugate Gradient	Resilence back-propagation	Tan-sigmoid	20	97.4%
		ReLU	24	99.9%
	Scaled Conjugate Gradient	Tan-sigmoid	32	98%
		ReLU	18	97.4%
	With Fletcher-Reeves Updates	Tan-sigmoid	45	99.9%
		ReLU	21	99.3%
	With Polak-Riebre Updates	Tan-sigmoid	15	98.5%
		ReLU	116	99.9%
Quasi Newton	BFGS	Tan-sigmoid	19	97.1%
		ReLU	18	97.1%
	Levenberg-Marquardt back-propagation	Tan-sigmoid	44	99%
		ReLU	13	99.6%
Bayesian Regularization	Bayesian Regularization Back-propagation	Tan-sigmoid	105	99.9%
		ReLU	66	99.9%

Figure 28 shows the average accuracy of classification against the number of hidden layers. Figure 29 shows the best performance during testing and training the network using ReLU activation function and Bayesian Regularization Back-propagation which gives the highest classification accuracy with two hidden layers (Reaches 99.9%) and figure 30 shows the Error Histogram.

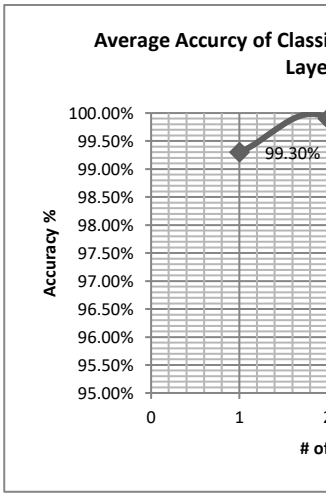

Fig. 28: Average Accuracy of Classification Against the Number of Hidden Layers.

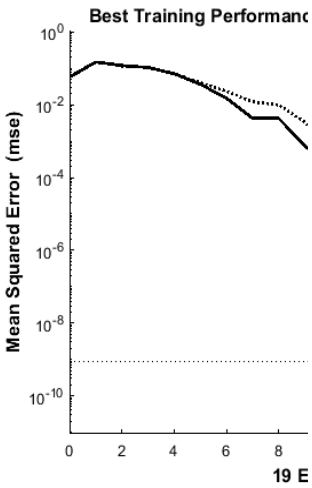

Fig. 29: Shows the Mean Squared Error VS. Iterations during Training and Testing the Network with Best Performance.

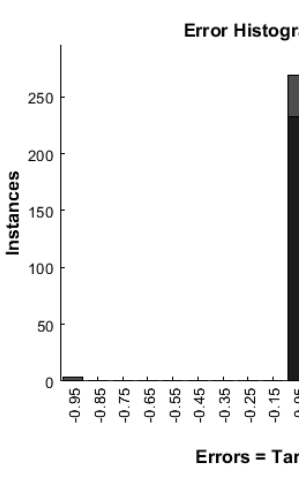

Fig. 30: Shows Error Histogram Diagram.

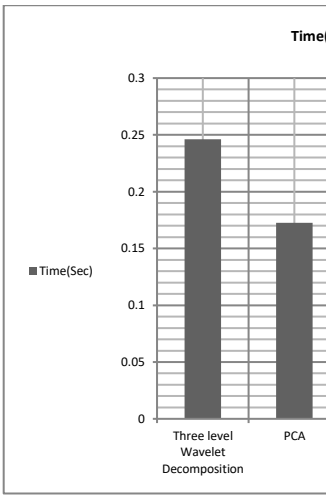

Fig. 31: Shows the Time Duration Spend by Each Step of the Classification Part (Classification, Final Features, GLCM, PCA and Wavelet Decomposition).

The following diagram in figure 31 shows the time duration taken by each step of the classification part:
Total Timing
Time durations spend by each process (Using a laptop with processor Intel(R) Core(TM) i3-6006U @2.00GHz 4GB RAM) is shown in table 4 .

Table 4: Shows the Time for Each Process

PROCESS	AVERAGE TIME(sec)
Histogram Processing	0.113399
Cranium Removal and Contrast Enhancement	0.343121
Morphological Operations	0.532167
Three level Wavelet Decomposition	0.246104
PCA	0.17247
GLCM	0.124524
Final Features Determination	0.279443
Classification Using KSVM	0.058446
Classification Using LDA	0.027627
ANN timing	1.463071

Figure 32 shows the percentage of total time taken by all processes for each step for the entire system.

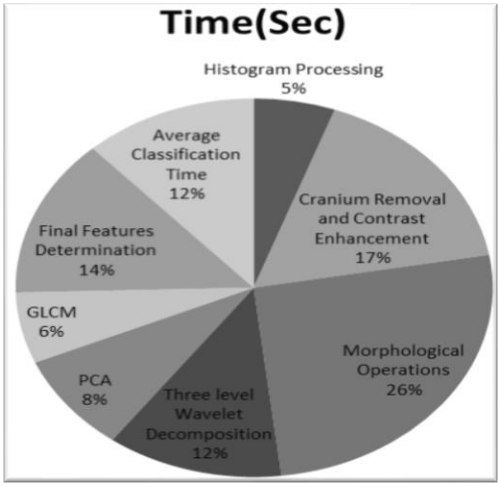

Fig. 32: Shows the Average Time Duration Spend by Each Step for All Steps.

5. Conclusion and future work

This paper presents a hybrid technique of brain tumor detection and classification using morphological operations , and this hybrid

technique consists of two main parts which are the segmentation part and the classification part, the segmentation part is tested before being used in the classification part as the segmentation is applied on the abnormal classification result MRI images , this segmentation part is executed through certain stages which are cranium removal ,histogram processing , morphological filtering ,segmentation and morphologically based post-processing stage , the result of this segmentation part is tested (as a primary test) on a collective scans from databases with average accuracy of 98.84% . The classification process which is a machine learning technique is executed through certain stages which are feature extraction using wavelet decomposition, feature reduction using Principal Component Analysis (PCA), extracting features from PCA output ,determining Gray Level Co-occurrence Matrix (GLCM) , extracting features from GLCM, extracting morphologically based additional features and fetching all the features to three techniques of classification which are SVM (Linear , using RBF kernel), LDA (Discriminant Classification) and ANN (as Pattern Recognition Feed-forward Multilayer Perceptron), this methodology of classification is tested on 274 slice image [21] of total 4110 features with average accuracy of 93.06%, 97.45% and 98.9% respectively , There are some future steps that could be used to improve the performance such as extracting more features, further testing on other databases, applying this technique on 3D images, applying this technique on frames after considering the minimum timing as a video processing brain tumor extraction and classification technique and also other types of neural network could be implemented to perform the task.

References

[1] Borole, V. Y., Nimbhore, S. S., & Kawthekar, D. S. S. (2015). Image Processing Techniques for Brain Tumor Detection: A Review. *International Journal of Emerging Trends & Technology in Computer Science (IJETTCS)*, *4*(5), 2.

[2] *Fact Sheets by Population*. (2018). *Globocan.iarc.fr*. Retrieved 4 October 2018, from http://globocan.iarc.fr/Pages/fact_sheets_population.aspx

[3] *Brain Tumor - Statistics*. (2012). *Cancer.Net*. Retrieved 4 October 2018, from https://www.cancer.net/cancer-types/brain-tumor/statistics

[4] Jeena, R. S., & Kumar, S. (2013, June). A comparative analysis of MRI and CT brain images for stroke diagnosis. In Emerging Research Areas and 2013 International Conference on Microelectronics, Communications and Renewable Energy (AICERA/ICMiCR), 2013 Annual International Conference on (pp. 1-5). IEEE. https://doi.org/10.1109/AICERA-ICMiCR.2013.6575935.

[5] Bauer, S., Wiest, R., Nolte, L. P., & Reyes, M. (2013). A survey of MRI-based medical image analysis for brain tumor studies. Physics in medicine and biology, 58(13), R97. https://doi.org/10.1088/0031-9155/58/13/R97.

[6] Bobotová, Z. Segmentation of Brain Tumors from Magnetic Resonance Images using Adaptive Thresholding and Graph Cut Algorithm.

[7] Deepthi Murthy TS, Sadashivappa G. Brain tumor segmentation using thresholding, morphological operations and extraction of features of tumor. International Conference on Advances in Electronics, Computers and Communications (ICAECC); Bangalore. 2014. p. 1-6.

[8] Halder, A., Pradhan, A., Dutta, S. K., & Bhattacharya, P. (2016, April). Tumor extraction from MRI images using dynamic genetic algorithm based image segmentation and morphological operation. In *Communication and Signal Processing (ICCSP), 2016 International Conference on* (pp. 1845-1849). IEEE. https://doi.org/10.1109/ICCSP.2016.7754489.

[9] Sharma, Manorama, G. N. Purohit, and Saurabh Mukherjee. "Threshold segmentation technique for tumor detection using morphological operator." *Communication and Computing Systems: Proceedings of the International Conference on Communication and Computing Systems (ICCCS 2016), Gurgaon, India, 9-11 September, 2016*. CRC Press, 2017.

[10] Maheshwari, D., Shah, A. A., Shaikh, M. Z., Chowdhry, B. S., & Memon, S. R. (2015). Extraction of Brain Tumour in MRI Images Using Marker Controlled Watershed Transform Technique in MATLAB. *Journal of biomedical engineering and medical imaging*, *2*(4), 9. https://doi.org/10.14738/jbemi.24.1260.

[11] Laddha, Roopali R., and S. A. Ladhake. "A Review on Brain Tumor Detection Using Segmentation And Threshold Operations." *International Journal of Computer Science and Information Technologies* 5.1 (2014): 607-611.

[12] Somasundaram, K., & Kalaiselvi, T. (2011). Automatic brain extraction methods for T1 magnetic resonance images using region labeling and morphological operations. *Computers in biology and medicine*, *41*(8), 716-725. https://doi.org/10.1016/j.compbiomed.2011.06.008.

[13] Somasundaram, K., & Kalaiselvi, T. (2010). Fully automatic brain extraction algorithm for axial T2-weighted magnetic resonance images. *Computers in biology and medicine*, *40*(10), 811-822. https://doi.org/10.1016/j.compbiomed.2010.08.004.

[14] El-Dahshan, E. S. A., Mohsen, H. M., Revett, K., & Salem, A. B. M. (2014). Computer-aided diagnosis of human brain tumor through MRI: A survey and a new algorithm. *Expert systems with Applications*, *41*(11), 5526-5545 https://doi.org/10.1016/j.eswa.2014.01.021.

[15] Zhang, Y., & Wu, L. (2012). An MR brain images classifier via principal component analysis and kernel support vector machine. *Progress In Electromagnetics Research*, *130*, 369-388. https://doi.org/10.2528/PIER12061410.

[16] Gupta, M., Rao, B. P., & Rajagopalan, V. (2016, December). Brain tumor detection in conventional MR images based on statistical texture and morphological features. In *Information Technology (ICIT), 2016 International Conference on* (pp. 129-133). IEEE.Y. Yorozu, M. Hirano, K. Oka, and Y. Tagawa, "Electron spectroscopy studies on magneto-optical media and plastic substrate interface," IEEE Transl. J. Magn. Japan, vol. 2, pp. 740–741, August 1987 [Digests 9th Annual Conf. Magnetics Japan, p. 301, 1982]. https://doi.org/10.1109/ICIT.2016.037.

[17] Sokolova, Marina, and Guy Lapalme. "A systematic analysis of performance measures for classification tasks." *Information Processing & Management* 45.4 (2009): 427-437. https://doi.org/10.1016/j.ipm.2009.03.002.

[18] Cheng, J., Huang, W., Cao, S., Yang, R., Yang, W., Yun, Z., ... & Feng, Q. (2015). Enhanced performance of brain tumor classification via tumor region augmentation and partition. *PloS one*, *10*(10), e0140381. https://doi.org/10.1371/journal.pone.0140381.

[19] Schölkopf, B., & Smola, A. J. (2002). *Learning with kernels: support vector machines, regularization, optimization, and beyond*. MIT press.

[20] Tharwat, A. (2016). Principal component analysis-a tutorial. *International Journal of Applied Pattern Recognition*, *3*(3), 197-240. https://doi.org/10.1504/IJAPR.2016.079733.

[21] The Whole Brain Atlas. (2018). Med.harvard.edu. Retrieved 25 March 2018, from http://www.med.harvard.edu/aanlib/home.html

[22] Fraz, M. M., Remagnino, P., Hoppe, A., & Barman, S. A. (2013, January). Retinal image analysis aimed at extraction of vascular structure using linear discriminant classifier. In Computer Medical Applications (ICCMA), 2013 International Conference on (pp. 1-6). IEEE. https://doi.org/10.1109/ICCMA.2013.6506180.